

INFRARED SPECTROSCOPY FROM SAN FERNANDO OBSERVATORY: He I 1083 nm, O I 1316 nm, AND Fe I 1565 nm

M. J. PENN, J. A. CEJA, E. BELL, G. FRYE and R. LINCK

San Fernando Observatory and California State University Northridge, Department of Physics and Astronomy, 18111 Nordhoff Street, Northridge, CA 91330-8268, U.S.A.

(Received 15 June 2001; accepted 22 August 2001)

Abstract. Imaging spectroscopy of the Sun was carried out at the California State University Northridge San Fernando Observatory using an InGaAs near-IR video camera. Using the Si I 1082.71 nm and He I 1083.03 nm lines the Evershed effect is measured simultaneously in the photosphere and the chromosphere for three sunspots; the speed of the Evershed flow is measured to be between 3 to 8 times greater in the He I line than in the Si I line, and the direction is radially inward in the chromosphere and outward in the photosphere. Telluric absorption lines prevented a meaningful measurement of O I 1128.7 nm limb emission, but an upper limit of $20 \times 10^{-3} B_{\odot}$ is measured for chromospheric limb emission at O I 1316.3 nm. Zeeman splitting in Fe I 1564.9 nm was observed in six sunspot umbrae, and a linear relationship between magnetic field and umbral continuum intensity is confirmed.

1. Introduction

Several instrument tests were done at the California State University Northridge (CSUN) San Fernando Observatory 61 cm Vacuum Telescope and Spectrograph (SFO-VT) using a Sensors Unlimited 128×128 pixel InGaAs near-IR camera borrowed from the National Solar Observatory on twelve dates from September 2000 through April 2001. Instrumental transmission measurements, performance tests of the normal incidence grating (Grating No. 3) and the Echelle grating (Grating No. 1) and pre-filter tests were made using imaging spectroscopy observations at several wavelengths from 1000 nm to 1600 nm. During the course of these tests several observations were taken that had scientific application, and the results from these measurements are presented herein.

The SFO-VT telescope and spectrograph have been described in detail (Mayfield *et al.*, 1969; Richter, 1985) and their use especially for spectropolarimetry at 630.3 nm has been recently described by Walton and Chapman (1996). Only the exit port of the spectrograph was modified for these observations; a small optical bench was attached and the InGaAs camera was mounted with a large amount of vertical travel available for focusing across the wavelength range observed. The video output signal from the InGaAs camera was digitized using a Matrox PULSAR frame grabber board in a Pentium-III PC running WinNT4.0 and the Matrox *Inspector32* software package. During observations, *Inspector32* wrote



between seven and eight frames per second to a PC disk digitized to 8-bits, in an uncompressed AVI format file while the telescope was moved to scan the image perpendicular to the spectrograph slit. The InGaAs camera covered about 129 arc sec along the slit at 1.01 arc sec per pixel (60 microns), and typical scans covered about 668 arc sec across the surface of the Sun at about 1.67 arc sec per step. The spectrograph slit ranged in size from 40 to 100 microns (0.67 to 1.7 arc sec), and the spectral dispersion varied roughly between 0.0089 nm (Grating No. 1) and 0.0122 nm (Grating No. 3) per pixel.

The data analysis was carried out at CSUN in two different ways; first using a set of PC computers running the Mathworks *Matlab* program (students), and also using RSI's *IDL* data reduction program on a UNIX-based machine (Penn). Several data analysis programs were written, including routines to read uncompressed AVI files into *Matlab* and *IDL*.

2. He I 1083 nm Data – Inverse Evershed Effect

The height variation of the Evershed flow, from an outwardly direct flow in the photosphere to an inwardly directed flow in the chromosphere, has been known since the early work of St. John (1913). Recent work of Rimmele (1995) shows that near the formation height of the Fe I 543.3 nm line (in the temperature minimum) the flow reverses direction. The speed of the inward flow velocity in the chromosphere was measured to be about the same value as the photospheric flows (St. John, 1913; Bønes and Maltby, 1978) when studied with the chromospheric lines of H I, Mg I, Na I and Ca II. However, by fitting simultaneous photospheric, chromospheric and transition region Doppler measurements with a flow model, Dere, Schmieder, and Alissandrakis (1990) find a steady increase in the magnitude of the Evershed radial velocity, with the chromospheric speed about twice the photospheric speed and the transition region speed (also inwardly directed) about ten times the photospheric speed.

The He I 1083.03 nm line offers another height diagnostic for measuring the chromospheric Evershed flow, and especially when used in conjunction with measurements of a strong neighboring photospheric line (Si I 1082.71 nm) important simultaneous multi-height flow measurements can be made to provide input to flow models (as in Alissandrakis *et al.*, 1988; and Dere, Schmieder, and Alissandrakis, 1990). While both Lites *et al.* (1985) and Lin (1997) mention that the Evershed effect appears normal in the photospheric Si I 1082.71 nm and reverses direction in the chromospheric He I 1083.03 nm, neither report the velocities measured with these lines.

Observations of NOAA 9169 were taken on 28 September 2000 from 22:38 to 23:36 UT while the region was near the solar limb ($r/R_{\odot} = 0.91$). Figure 1 shows a sample spectral frame at the He I 1083.03 nm line; one of the several umbrae in NOAA 9169 is visible with a dark continuum, and Doppler velocities in the

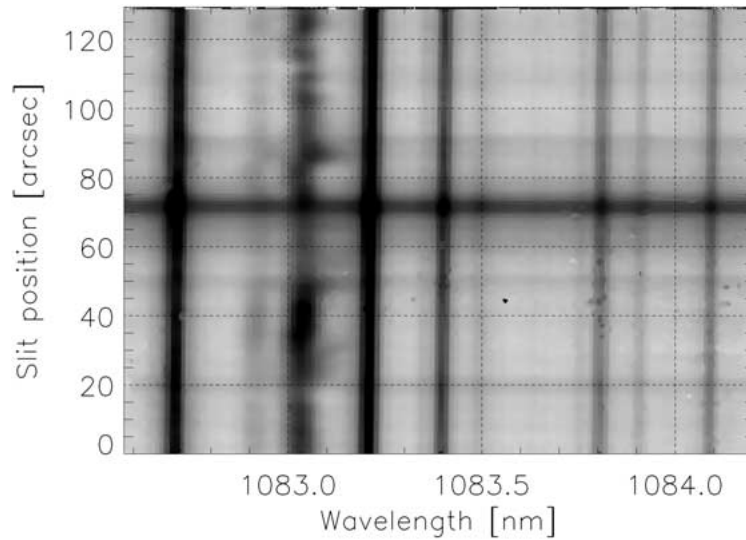


Figure 1. A spectral frame of the He I 1083.03 nm line from observations taken on 28 September 2000 of region NOAA 9169. One umbra of the region crossing the slit at position 72 arc sec can be seen as a dark horizontal streak. Evidence of Evershed flow in the penumbra at slit position 78 arc sec is visible in the Si I 1082.71 nm and He I 1083.03 nm lines. Strong red shifts are also seen in the He I 1083.03 nm at other slit positions.

He I 1083.03 nm line are visible along the entire spectrograph slit. On 30 April 2001 imaging spectroscopy observations at the He I 1083.03 nm line were made of NOAA 9433 ($r/R_{\odot} = 0.90$), NOAA 9436 ($r/R_{\odot} = 0.70$), and NOAA 9441 ($r/R_{\odot} = 0.01$) from roughly 22:00 to 23:30 UT. Although no Evershed flow signal can be seen in the disk-center region NOAA 9441, this region was observed in order to measure the systematic errors in the analysis.

The data were calibrated and Doppler velocity maps were produced using both Si I 1082.71 nm and He I 1083.03 nm. The Doppler maps from 6 to 10 scans (covering 15 to 20 minutes of time) of a spot region were averaged to remove solar velocity oscillations. The solar rotation signal was removed and the Doppler maps were corrected for solar limb position, assuming a horizontal flow field only. The average velocity was calculated across the penumbra of each spot, using intensity thresholds and the radial distance from the spot center to define the penumbral regions. Figure 2 shows the Doppler velocity in both the Si I 1082.71 nm and the He I 1083.03 nm lines plotted versus azimuth angle for observations of NOAA 9436. The direction toward the solar limb is near $\pm \pi$ radians. The velocity data are binned in azimuth; the large points in Figure 2 show the mean value within each bin, and the error bars show the standard deviation. A pair of sine curves are then fit to the binned data with a least squares procedure where the phase shift between the two curves is forced to be π radians to represent the inward and outward flow directions seen in the two different lines. Unlike Alissandrakis *et al.* (1988) no

TABLE I
Evershed flow observations

NOAA region	Silicon speed (km s ⁻¹)	Helium speed (km s ⁻¹)	Ratio
9169	0.2 ± 0.1	1.3 ± 0.1	6.5 ± 0.8
9433	0.4 ± 0.1	1.3 ± 0.1	3.3 ± 0.4
9436	0.3 ± 0.1	2.2 ± 0.1	7.3 ± 0.8

vertical sunspot velocity fields are considered in this simple model. Figure 2 shows the best fit curves for NOAA 9436, and the fit values for this spot and the others are listed in Table I. The speed measured in the Si I 1082.71 nm line compares favorably to lines formed in the upper photosphere but it is slower than typical photospheric lines used to study Evershed flow, such as the Fe I 617.3 nm line used by Dere, Schmieder, and Alissandrakis (1990). While the Evershed study of Degenhardt and Wiehr (1994) found that the Si I 614.5 nm line was formed slightly below the Fe I 557.6 nm line, no calculations of the formation height for the Si I 1082.71 nm line have been made and so it is assumed to be formed in the high photosphere. The He I 1083.03 nm line speeds are consistent with chromospheric measurements, for instance from Ca II K_2 and K_3 (St. John, 1913) and the wings of H α (Dere, Schmieder, and Alissandrakis, 1990); the quiet-Sun heights of formation for Ca II K_2 and K_3 (Vernazza, Avrett, and Loeser, 1981) are near to the measured limb height for the He I 1083.03 nm of 1.74 Mm (Penn and Jones, 1996).

As seen by Dere, Schmieder, and Alissandrakis (1990) spurious velocities which are not fit well with a simple Evershed flow model are seen at particular azimuth angles in the penumbra in these observations, sometimes with velocities of several km s⁻¹. However, there is also a systematic error, perhaps due to incomplete removal of solar oscillations, demonstrated by observations of an amplitude of 0.1 km s⁻¹ in the disk center NOAA 9441 data. This value is used as an error estimate in the calculation of the velocity ratio presented in the last column of Table I. The Evershed flow field shows a speed in the He I 1083.03 nm line of between 3 to 8 times the speed observed in the Si I 1082.71 nm line, as well as the reversal in the direction of the flow seen in the two lines.

3. Search for Near-IR O I lines

Production of the spectrum of O I on the Sun is thought to involve both collisional processes and a mechanism called photoexcitation by accidental resonance (PAR). The PAR mechanism is a pumping process whereby O I electrons are excited due to the accidental energy proximity of an oxygen transition with the strong solar

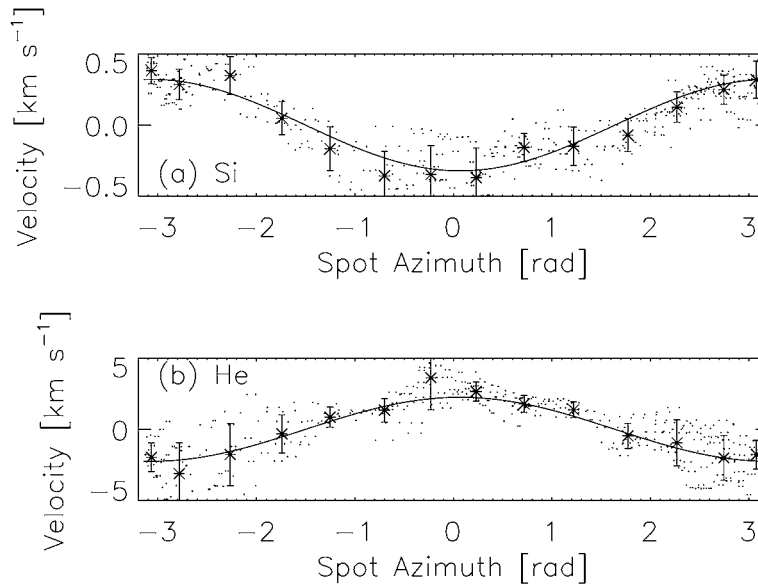


Figure 2. Measurements of the Evershed flow from (a) the Si I 1082.71 nm line and the inverse Evershed flow from the (b) He I 1083.03 nm line from observations of NOAA 9436 on 30 April 2001. *Small points* show the velocity measured in individual penumbral pixels versus the azimuth angle from the spot center (the solar limb is toward $\pm\pi$ radians). The data are binned in azimuth; the *large points* show the mean velocity and the *error bars* show the standard deviation within each bin. A simple horizontal radial flow model is fit to the data using a sine curve, with a phase change of π radians between the Si I 1082.71 nm and He I 1083.03 nm lines. The resulting fits from three spots are listed in Table I.

H I Lyman- β emission line at 102.6 nm. Measurements of the O I limb emission lines at 777.4 and 844.6 nm from eclipse data (Athay and Judge, 1995) and from non-eclipse measurements (Penn, 1999) suggest the PAR mechanism plays only a limited role in the O I emission, and that O I lines are formed in regions with high electron number density (N_e), particularly where $N_e > 10^{11.5}\text{cm}^{-3}$. However, as discussed by Kastner (1995), a set of near infrared oxygen lines provide the best tool to test the importance of the PAR process. The O I line at 1128.7 nm is the first transition out of the PAR excited $3d(^3D^0)$ state, and a line at 926.4 nm is the first transition out of the $3d(^5D)$ state, which is not populated by the PAR mechanism. Comparing the emission in these two O I lines would provide a direct constraint on the PAR process.

However, since the 926.4 nm line is below the short wavelength cutoff for the NSO InGaAs camera, a different approach was used. Downward transitions from $3d(^3D^0)$ at 1128.7 nm populate the $3p(^3P)$ level (see Kastner and Bhatia, 1995; Figure 1). Cascades out of this $3p(^3P)$ level occur through the 844.6 nm line to the $3s(^3S^0)$ state. However, also feeding the $3p(^3P)$ level are transitions from $4s(^3S^0)$ through the 1316.3 nm transition. By comparing the emission in 1128.7 nm (PAR electrons) to that in 1316.3 nm (non-PAR electrons) and particularly comparing

the line emission to the known 844.6 nm emission strength (about 10^{-2} of the disk center intensity, Penn, 1999) another measurement of the importance of the PAR mechanism in the O I solar spectrum can be obtained. Since both 1128.7 nm and 1316.3 nm lie in the wavelength range of the InGaAs camera, observations of these lines were taken.

On 10 October 2000 limb spectra were taken at SFO-VT examining the solar spectrum near 1129 nm. Unfortunately, unexpectedly strong telluric absorption lines were present in these observations. The SFO-VT spectra show somewhat deeper telluric absorption than seen from Kitt Peak (Livingston and Wallace, 1991), and due to the strength of the telluric absorption a meaningful upper limit on the O I 1128.7 nm emission can not be determined. Telluric lines do not interfere with observations at O I 1316.3 nm. If the O I 1316.3 nm limb emission behaves like the 777.4 and 844.6 nm emission, the O I lines should show emission from 3 to 5 arc sec above the solar limb (Penn, 1999). No emission is seen in the SFO-VT data. An average of 400 limb spectral frames showed a noise level of about $\pm 7 \times 10^{-3}$ of the disk center intensity (B_{\odot}), primarily due to residual fringes caused by difficulty in flat fielding the InGaAs array because of its non-linear response. Simulations with the data confirmed that a line emission with the expected spatial and spectral properties of the O I emission at 1316.3 nm with an intensity of $20 \times 10^{-3} B_{\odot}$ (three times the noise level) would have been easily detected in these measurements, and so this is the upper limit for O I 1316.3 nm emission given by these observations.

4. Fe I 1565 nm Data – Zeeman Splitting and Sunspot Continuum Intensity

Spectropolarimetric observations of the $g = 3$ Fe I 1564.9 nm line have been made by several groups (McPherson, Lin, and Kuhn, 1992; Kopp and Rabin, 1992, and recently by Bellot Rubio *et al.*, 2000). The line provides more sensitivity to the magnetic Zeeman effect than visible absorption lines due to its large g factor and its location at near-infrared wavelengths; in sunspots the Zeeman splitting of the Fe I 1564.9 nm line is fully resolved since the Zeeman shift is larger than the Doppler line width. The solar magnetic field (B , in gauss) can be measured from the splitting of the Fe I 1564.9 nm line following Equation 1 from McPherson, Lin, and Kuhn (1992) as $B = 2.86 \times 10^4 \Delta\lambda$ where $\Delta\lambda$ is the wavelength shift of the Zeeman component from line center (nm).

Imaging spectroscopic observations (Stokes I) of Fe I 1564.9 nm were made on 16, 23 and 27 April 2001 at SFO-VT, since currently SFO-VT has no polarimeter which operates at this wavelength. The active region NOAA 9429 was observed on 16 April, NOAA 9432, 9433, 9435 and 9436 were observed on 23 April, and NOAA 9433, 9435 and 9436 were observed on 27 April. The most obvious Zeeman splitting was seen in NOAA 9433 on 23 April, and Figure 3 shows a Stokes I spectral frame which includes the sunspot umbra. In Figure 3, the continuum variations have been removed with a polynomial fit, enhancing the Zeeman splitting. (The

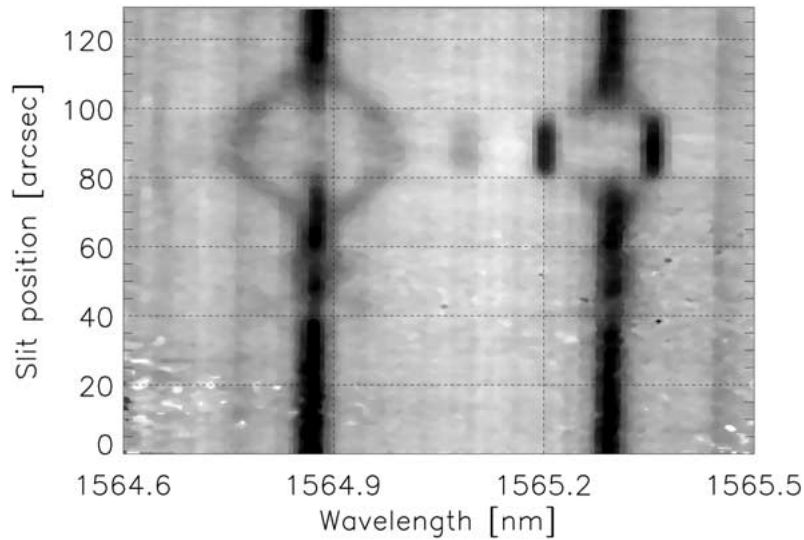


Figure 3. A Stokes I spectrum of the large umbra in NOAA 9433 from 23 April 2001 observations at Fe I 1564.9 nm. The continuum intensity has been removed with polynomial fits, but the sunspot umbra covers slit position 80 to 100 arc sec, with about 10 arc sec of penumbra on either side. The $g = 3$ Fe I line at 1564.9 nm shows strong Zeeman splitting and implies a total magnetic field of 2.9×10^3 G. Three strong umbral absorption lines from the OH molecule are also visible.

umbra of the spot extends roughly from slit position 80 to 100 arc sec, and the penumbra from about 70 to 80, and from 100 to 110 arc sec.) Zeeman splitting is visible in the Fe I lines present in the spectral frame at 1564.9 nm and 1565.3 nm; strong molecular OH lines (Wallace and Livingston, 1992) are visible in the umbra at about 1565.1 nm, 1565.2 and 1565.35 nm. From Figure 3, the shift of the Zeeman components can be estimated to be about 0.1 nm, implying the magnetic field of the umbra of NOAA 9433 was about 2.9×10^3 G. These Stokes I spectra measure the absolute value of the total magnetic field strength independent of the view angle to the sunspot umbra.

As noted by Kopp and Rabin (1992), the continuum intensity at 1565 nm is a good indicator of the plasma temperature, and with low scattered light at this wavelength in most telescopes, it is natural to compare the magnetic field measured with the $g = 3$ Fe I 1564.9 nm line to the continuum intensity to explore the physical relation of magnetic field and temperature in and around sunspots. A linear behavior between B and umbral intensity was found by Kopp and Rabin (1992), roughly consistent with magneto-hydrostatic equilibrium in a vertical magnetic field.

The Zeeman splitting in the SFO-VT data is measured for six umbrae (including NOAA 9432, the three large umbra in NOAA 9433, the westernmost umbra of NOAA 9435 and NOAA 9436) on 23 April 2001. The spectral data cubes are binned to three arc sec square pixels, and Gaussian fits to the blue and red components are made in the umbral regions of each spot group, which are defined

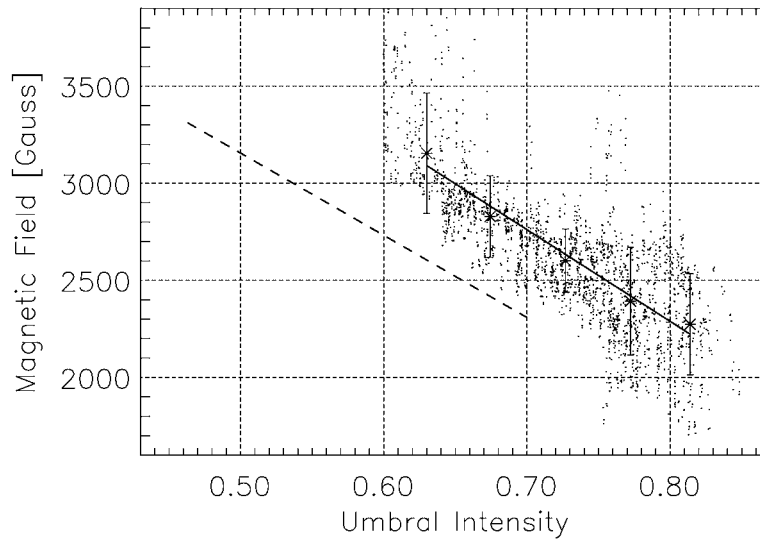


Figure 4. The umbral intensity (normalized by the quiet Sun) versus the total magnetic field is plotted for six sunspot umbrae; binned data are shown as *large points*, and a linear fit to the binned data is shown as a *solid line*. Measurements from Kopp and Rabin (1992) are shown as the *dashed line*. While the line slopes are identical within measurement error, the continuum intensity offset between the two lines is likely due to a larger stray light contamination in the SFO-VT data.

by continuum thresholds determined by the nearby continuum intensity. The raw umbral continuum intensity is normalized by the intensity of the nearby photosphere. The magnetic field measured is plotted with umbral continuum intensity in Figure 4. Individual umbral measurements are shown as small dots and the scatter in the data is consistent with the measurement error, estimated by comparing the different measured shifts of the red and blue components in a few sample spectra. The data are binned (*large points*) and fit with a linear relationship as shown with the *solid line*; the error bars on the *large points* show the standard deviation within each bin. Also shown in Figure 4 is a *dashed line* representing the locus of umbral measurements from Kopp and Rabin (1992). The SFO-VT data show a very similar linear relationship, although with brighter umbral intensities for a given magnetic field strength. The umbrae studied by Kopp and Rabin were selected to be near the center of the solar disk with values of μ greater than 0.75 whereas the umbrae studied from the SFO-VT data were closer to the limb (with values of μ ranging from 0.59 to 0.32) and thus had smaller projected areas. While a simple stray-light correction has been made to the SFO-VT data (correcting for the 1% measured sky background), the grating used for these measurements (Grating No. 1) suffers from astigmatism, which has the effect of placing the spectrograph slit outside of the image focal plane. It is likely that uncorrected stray light from this unfocused slit combined with the smaller umbral areas of the SFO-VT targets is the source of the intensity difference.

Acknowledgements

MJP would like to thank G. Chapman, S. Walton, and R. Rideout for help at the SFO-VT and S. Keil at NSO for the loan of the InGaAs camera. MJP would also like to thank P. Mein for providing valuable referee comments. This work was made possible by the NSF grant ATM 0077624 which provided salary support for the CSUN undergraduate students involved in this project.

References

- Alissandrakis, C. E., Dialets, D., Mein, P., Schmieder, B. and Simon, G.: 1988, *Astron. Astrophys.* **201**, 339.
- Athay, R. G. and Judge, P. G.: 1995, *Astrophys. J.* **438**, 491.
- Bellot Rubio, L. R., Collados, M., Cobo, R., and Rodríguez Hidalgo, I.: 2000, *Astrophys. J.* **534**, 989.
- Bønes, J. and Maltby, P.: 1978, *Solar Phys.* **57**, 65.
- Degenhardt, D. and Wiehr, E.: 1994, *Astron. Astrophys.* **287**, 620.
- Dere, K. P., Schmieder, B., and Alissandrakis, C. E.: 1990, *Astron. Astrophys.* **233**, 207.
- Kastner, S. O., 1995, in J. R. Kuhn and M. J. Penn (eds.), *Infrared Tools for Solar Astrophysics: What's Next?*, Singapore, World Scientific, p 55.
- Kastner, S. O. and Bhatia, A. K.: 1995, *Astrophys. J.* **439**, 346.
- Kopp, G. and Rabin, D.: 1992, *Solar Phys.* **141**, 253.
- Lites, B. W., Keil, S. L., Scharmer, G. B., and Wyller, A. A.: 1985, *Solar Phys.* **97**, 35.
- Lin, H.: 1997, *BAAS Abstract* **28**, No. 17.03
- Livingston, W. and Wallace, L.: 1991, *An Atlas of the Solar Spectrum in the Infrared from 1850 to 9000 cm⁻¹ (1.1 to 5.4 microns)*, N.S.O. Technical Report No. 91-001.
- Mayfield, E. B., Vrabec, D., Rogers, E. H., Janssens, T. J., and Becker, R. A.: 1969, *Sky and Telescope*, **37**, 208.
- McPherson, M. R., Lin, H., and Kuhn, J. R.: 1992, *Solar Phys.* **139**, 255.
- Penn, M. J.: 1999, *Astrophys. J.* **518**, L131.
- Penn, M. J. and Jones, H. P.: 1996, *Solar Phys.* **168**, 19.
- Richter, P. 1985, in M. J. Hagyard (ed.), *Measurements of Solar Vector Magnetic Fields*, NASA Conf. Publ. 2374, 202.
- Rimmele, T. R.: 1995, *Astron. Astrophys.* **298**, 260.
- St. John, C. E.: 1913, *Astrophys. J.* **37**, 322.
- Vernazza, J. E., Avrett, E. H., and Loeser, R.: 1981, *Astrophys. J. Suppl. Ser.* **45**, 635.
- Wallace, L. and Livingston, W.: 1992, *An Atlas of a Dark Sunspot Umbral Spectrum from 1970 to 8640 cm⁻¹ (1.16 to 5.1 microns)*, N.S.O. Technical Report No. 92-001.
- Walton, S. R. and Chapman, G. A.: 1996, *Solar Phys.* **166**, 267.